2164. An improved Fourier series method for vibration analysis of moderately thick annular and circular sector plates subjected to elastic boundary conditions

Fazl e Ahad[1], Dongyan Shi[2], Zarnab Hina[3], Syed M. Aftab[4], Hafiz M. Waqas[5]
[1, 2, 4, 5]College of Mechanical and Electrical Engineering, Harbin Engineering University, Harbin, China
[3]College of Information and Communication Engineering, Harbin Engineering University, Harbin, China
[1]Corresponding author
E-mail: [1]*ahad_khattak@hotmail.com*, [2]*shidongyan@hrbeu.edu.cn*, [3]*zarnabhina@gmail.com*,
[4]*s.mohammadaftab@hotmail.com*, [5]*hafizwaqas90@hotmail.com*

Abstract. In this paper, an improved Fourier series method is presented for vibration analysis of moderately thick annular and circular sector plates subjected to general elastic boundary conditions along its edges. In literature, annular and circular sector plates subjected to classical boundary conditions have been studied in detail however in practical engineering applications the boundary conditions are not always classical in nature. Therefore, study of vibration response of these plates subjected to general elastic boundary conditions is far needed. In the method presented, artificial boundary spring technique has been employed to simulate the general elastic boundary conditions and first order shear deformation theory has been employed to formulate the theoretical model. Irrespective of the boundary conditions, each of the displacement function is expressed as a new form of trigonometric expansion with accelerated convergence. Rayleigh-Ritz method has been employed to determine the expansion coefficients. Unlike most of the studies on vibration analysis of moderately thick annular sector plates, the present method can be universally applied to a wide range of vibration problems involving different boundary conditions, varying material and geometric properties without modifying the solution algorithms and procedure. The effectiveness, reliability and accuracy of the present method is fully demonstrated and verified by several numerical examples. Bench mark solutions for moderately thick annular sector and circular plates under general elastic boundary conditions are also presented for future computational methods.

Keywords: vibrations, circular plates, annular plates, sector plates, natural frequency, mode shapes, arbitrary boundary conditions.

1. Introduction

Annular, circular and their sector parts are key structural components that are used in various engineering fields like civil, marine, aerospace and mechanical engineering. Due to different geometrical shapes of these structures, they have been analyzed separately using different solution techniques. Most of the initial research on these plates was done using Classical plate theory (CPT) in which the shear deformation and rotary inertia was neglected which in turn limited its application on moderately thick and thick plates. Later a lot of theories were proposed incorporating the shear deformation and rotary inertia which resulted in an increase in accuracy of the results for moderately thick and thick annular and circular plates. These theories' have been well explained in Leissa's book on vibration of plates.

Different methods have been employed by various researchers to study the vibration characteristics of annular and circular plates subjected to different boundary conditions. However, a few prominent studies related to these plates are highlighted here in this manuscript. Employing the Mindlin plate theory on thick sector plates, Guruswamy et al. [1] studied the dynamic response of these plates by proposing a sector finite element. Fully clamped boundary conditions were employed on all edges. Taking the effect of shear deformation in thickness direction, another study was performed by Soni et al. [2] on axisymmetric non uniform circular disks. In their research

they employed Chebyshev collocation technique to study the vibration characteristics of these plates. In another study Rayleigh-Ritz method was employed by Liew et al. on circular plates with multiple internal ring supports. Later in another study they studied the characteristics of these plates subjected to in-plane pressure [3-4].

Using three dimensional finite strip model, thick and thin sector plates subjected to various combinations of classical boundary condition were analyzed by Cheung et al. [5]. The integral equation technique and finite strip method was employed by Sirinivasan et al. and Misuzawa et al. respectively to study the vibration characteristics of Mindlin annular sector plates [6-7]. Employing the Mindlin plate theory and differential quadrature method, Liu et al. studied the effect of sector angle and thickness to radius ratio on the vibration characteristics of moderately thick sector plates [8]. Later they extended the same differential quadrature method to annular sector plates having shear deformation subjected to different combinations of classical boundary conditions [9]. In another study, the same differential quadrature method was employed on solid circular plates with variable thickness in radial direction and subjected to elastic boundary conditions by Wu et al. [10]. Similarly, Xiang et al. employed domain decomposition technique and studied the vibration response of circular plates with stepped thickness variation [11].

Using Rayleigh-Ritz method So et al. [12] studied the vibration characteristics of annular and circular plates by employing three dimensional elasticity theory. A similar three dimensional study was performed by Hashemi et al. on annular sector plates resting on elastic foundations. He employed polynomial-Ritz approach and studied the vibration characteristics for different sets of classical boundary conditions [13]. In another study similar polynomial-Ritz model was presented by Liew et al. to investigate the effect of boundary conditions and thickness on the vibration characteristics of annular plates [14]. In another prominent three dimensional study Chebyshev-Ritz technique was employed on circular and annular plates by Zhou et al. to study the vibration characteristics of these plates [15]. In plane vibrations of circular plates subjected to different boundary conditions were investigated by various researchers using different solution techniques [16-17]

From the studies mentioned above it can be seen that most of the previous studies on annular and circular plates were limited to classical boundary conditions which includes free, simply supported, clamped or combination of these. However, in practical engineering applications the boundary conditions are not always classical in nature. Therefore, the development of an analytical method universally dealing with arbitrary boundary conditions was much needed. An improved Fourier series method was developed for vibration analysis of beams and plates by Li [18-22]. Later Xianjie Shi et al. extended this method to thin annular plates to study its vibration characteristics [23-26]. The main objective of this study is to realize and extend the same generalized Fourier series method to study the vibration analysis of Mindlin annular sector and circular sector plates under various boundary conditions including the general elastic restraints.

2. Theoretical formulation

2.1. Model description

Consider an annular sector plate of constant thickness h, inner radius a, outer radius b and width R in radial direction as shown in Fig. 1. The plate geometry and dimensions are defined in the cylindrical coordinate system (r, ϕ, z). A local coordinate system (s, ϕ, z) is also shown in Fig. 1. The radial and thickness coordinates s and z are measured normally from the inner edge and mid plane of the annular sector plate respectively whereas ϕ is the circumferential angle. Four sets of distributed springs (one translational and two rotational) of arbitrary stiffness values are attached at each edge to simulate arbitrary boundary conditions. All the classical sets of boundary conditions can easily be achieved by varying the stiffness value of each spring from zero to an infinitely large number i.e. 10^{14}.

The domain of the annular sector plate can be defined as:

$$0 \leq s \leq R, \quad (R = b - a), \quad -\frac{h}{2} \leq z \leq \frac{h}{2}, \quad 0 \leq \phi < 2\pi, \tag{1}$$

The relationship between local and global coordinate system can be expressed as:

$$s = r - a. \tag{2}$$

The material of the plate is assumed to be isotropic with material density ρ, young's modulus E and Poisson ratio v. It should be noted that a circular sector plate can be defined as a special case of an annular sector plate if the inner radius 'a' is set either equal to 0 or to a very small number say 0.00001.

The displacement field of Mindlin annular sector plate in cylindrical coordinates is given by:

$$\begin{aligned}
u_r(r, \phi, z, t) &= u_r(r, \phi, z) + z\theta_r(r, \phi, t), \\
u_\phi(r, \phi, z, t) &= u_\phi(r, \phi, z) + z\theta_\phi(r, \phi, t), \\
w(r, \phi, z, t) &= w_o(r, \phi, t),
\end{aligned} \tag{3}$$

where z is the thickness coordinate, u_r and u_ϕ are displacements of the mid plane in r and ϕ directions, respectively, w is the transverse displacement. θ_r and θ_ϕ are the rotation functions of the middle surface and t is the time. Assuming the plain stress distribution in accordance with Hooks law, the stress resultants are obtained for Mindlin annular plate by integrating the stresses as shown below:

$$M_{rr} = \int_{-h/2}^{h/2} \sigma_{rr}\, z dz = \int_{-h/2}^{h/2} \frac{E}{(1-v^2)}(\varepsilon_{rr} + v\varepsilon_{\phi\phi})\, z dz = D\left[\frac{\partial\theta_r}{\partial r} + \frac{v}{r}\left(\theta_r + \frac{\partial\theta_\phi}{\partial\phi}\right)\right],$$

$$M_{\phi\phi} = \int_{-h/2}^{h/2} \sigma_{\phi\phi}\, z dz = \int_{-h/2}^{h/2} \frac{E}{1-v^2}(\varepsilon_{\phi\phi} + v\varepsilon_{rr})z dz = D\left[\frac{1}{r}\left(\theta_r + \frac{\partial\theta_\phi}{\partial\phi}\right) + v\left(\frac{\partial\theta_r}{\partial r}\right)\right],$$

$$M_{r\phi} = \int_{-h/2}^{h/2} \tau_{r\phi}\, z dz = \int_{-h/2}^{h/2} G\gamma_{r\phi}\, z dz = D\left(\frac{1-v}{2}\right)\left[\frac{1}{r}\left(\frac{\partial\theta_r}{\partial\phi} - \theta_\phi\right) + \frac{\partial\theta_\phi}{\partial r}\right], \tag{4}$$

$$Q_{rr} = K^2 \int_{-h/2}^{h/2} \tau_{rz}\, dz = K^2 Gh\left[\theta_r + \frac{\partial w_o}{\partial r}\right],$$

$$Q_{\phi\phi} = K^2 \int_{-h/2}^{h/2} \tau_{\phi z}\, dz = K^2 Gh\left[\theta_\phi + \frac{1}{r}\frac{\partial w_o}{\partial\phi}\right],$$

where M_{rr}, $M_{\phi\phi}$ and $M_{r\phi}$ are the bending moments per unit length of the plate, Q_{rr} and $Q_{\phi\phi}$ are the transverse shear forces per unit length of the plate, σ_{rr}, $\sigma_{\phi\phi}$ are the normal stresses, and $\tau_{r\phi}$, τ_{rz} and τ_{rz} are the shear stresses, h is the plate thickness, E is the modulus of elasticity, G is the shear modulus, v is the Poisson ratio, $D = Eh^3/12(1 - v^2)$ is the flexural rigidity and $K = \pi^2/12$ is the shear correction factor to compensate for the error in assuming the constant shear stress throughout the plate thickness.

The equation of motion of Mindlin plates in (r, ϕ, z) is given by:

$$\frac{\partial M_{rr}}{\partial r} + \frac{1}{r}\frac{\partial M_{r\phi}}{\partial \phi} + \frac{1}{r}\left(M_{rr} - M_{\phi\phi}\right) - Q_{rr} = \frac{\rho h^3}{12}\left(\frac{\partial^2 \theta_r}{\partial t^2}\right),$$

$$\frac{\partial M_{r\phi}}{\partial r} + \frac{1}{r}\frac{\partial M_{\phi}}{\partial \phi} + \frac{2}{r}M_{r\phi} - Q_{\phi\phi} = \frac{\rho h^3}{12}\left(\frac{\partial^2 \theta_\phi}{\partial t^2}\right), \tag{5}$$

$$\frac{\partial Q_{rr}}{\partial r} + \frac{1}{r}\frac{\partial Q_{\phi\phi}}{\partial \phi} + \frac{Q_{rr}}{r} = \rho h \frac{\partial^2 w_o}{\partial t^2}.$$
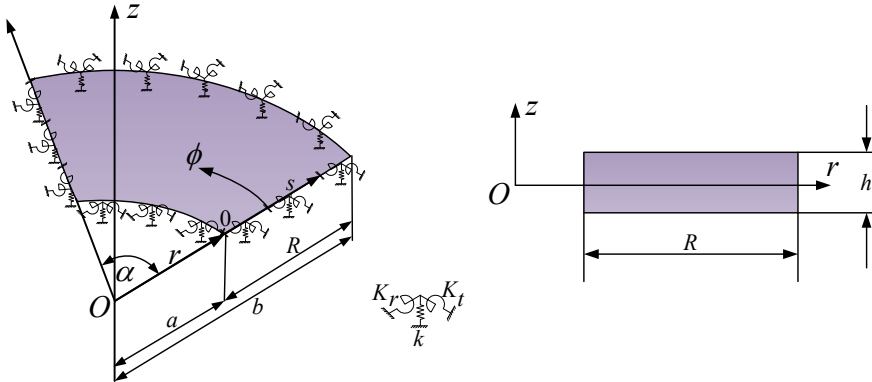

Fig. 1. Mindlin sector plate geometry

2.2. Solution scheme

2.2.1. Selection of admissible displacement function

Assume that the displacement field of Mindlin annular sector plate in local coordinate system (s, ϕ, z) is defined by the following series:

$$\theta_{s(s,\phi)} = \sum_{m=n=-2}^{\infty} A_{mn}\, \varphi_m(s)\varphi_n(\phi), \quad (r = s + a),$$

$$\theta_{\phi(s,\phi)} = \sum_{m=n=-2}^{\infty} B_{mn}\varphi_m(s)\varphi_n(\phi), \tag{6}$$

$$w_{o(s,\phi)} = \sum_{m=n=-2}^{\infty} C_{mn}\varphi_m(s)\varphi_n(\phi),$$

where:

$$\varphi_m(s) = \begin{cases}\cos\lambda_m(s), & m \geq 0 \\ \sin\lambda_m(s), & m < 0\end{cases}, \quad \varphi_n(\phi) = \begin{cases}\cos\lambda_n(\phi), & n \geq 0 \\ \sin\lambda_n(\phi), & n < 0\end{cases}$$

and $\lambda_m = m\pi/R$, $\lambda_n = n\pi/\alpha$ and A_{mn}, B_{mn}, C_{mn} denotes the Fourier series expansion coefficients. The sine terms in the equations Eq. (6) are introduced to overcome the potential discontinuities (convergence problem) of the displacement function, along the edges of the plate, when it is periodically extended and sought in the form of trigonometric series expansion. The addition of these auxiliary functions in the admissible functions plays an important role in the convergence and accuracy of the present method or in other words the elimination of potential discontinuities at the ends or elimination of Gibbs effect.

In order to illustrate this, take a beam problem for example. The governing equations for free vibration of a general supported Euler beam is obtained as:

$$D\frac{\partial^4 w(x)}{\partial x^4} - \rho A \omega^2 w(x) = 0, \tag{7}$$

where D, ρ and A are, respectively, the flexural rigidity, the mass density and the cross sectional area of the beam, and ω is frequency in radian. From Eq. (7) it can be observed that the displacement solution $w(x)$ on a beam of length L is required to have up to the fourth derivatives, that is, $w(x) \in C^3$. In general, the displacement function $w(x)$ defined over a domain $[0, L]$ can be expanded into a Fourier series inside the domain excluding the boundary points:

$$w(x) = \sum_{m=0}^{\infty} A_m \cos\left(\frac{m\pi x}{L}\right), \tag{8}$$

where A_m are the expansion coefficients. From the Eq. (8), we can see that the displacement function $w(x)$ can be viewed as a part of an even function defined over $[-L, L]$, as shown in Fig. 2.
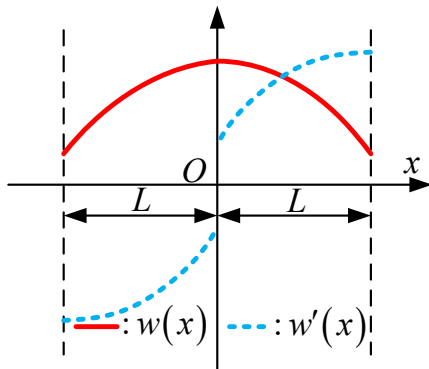

Fig. 2. An illustration of the possible discontinuities of the displacement at the end points
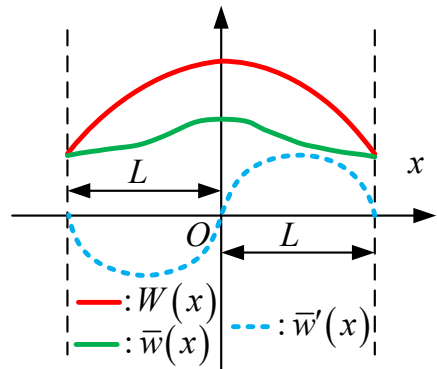

Fig. 3. An illustration of removal of possible discontinuities (convergence problem) at ends

Thus, the Fourier cosine series is able to correctly converge to $w(x)$ at any point over $[0, L]$. However, its first-derivative $w'(x)$ is an odd function over $[-L, L]$ leading to a jump at end locations. The corresponding Fourier expansion of $w'(x)$ continue on $[0, L]$ and can be differentiated term-by-term only if $w(0) = w(L) = 0$. Thus, its Fourier series expansion (sine series) will accordingly have a convergence problem due to the discontinuity at end points (Gibbs phenomena) when $w'(x)$ is required to have up to the first-derivative continuity.

To overcome this problem, this Improved Fourier Series technique was proposed by Li [18, 19]. In this technique a new function $P(x)$ is considered in the displacement function:

$$\bar{w}(x) = W(x) + P(x) = \sum_{m=0}^{\infty} A_m \cos\left(\frac{m\pi x}{L}\right) + P(x), \tag{9}$$

where the auxiliary function $P(x)$ in equation above represents an arbitrary continuous function that, regardless of boundary conditions, is always chosen to satisfy the following equations:

$$P' = w'(0), \quad P'(L) = w'(L), \quad P'''(0) = w'''(0), \quad P'''(L) = w'''(L). \tag{10}$$

The actual values of the first and third derivatives (a sine series) at the boundaries need to be determined from the given boundary conditions. Essentially, $\bar{w}(x)$ represents a residual beam function which is continuous over $[0, L]$ and has zero slopes at the both ends, as shown in Fig. 3.

Apparently, the cosine series representation of $\bar{w}(x)$ is able to converge correctly to the function itself and its first derivative at every point on the beam.

Thus, based on the above analysis, $P(x)$ can be understood as a continuous function that satisfies Eq. (9), and its form is not a concern but must be a closed-form and sufficiently smooth over a domain $[0, L]$ of the beam in order to meet the requirements provided by the continuity conditions and boundary constraints. Furthermore, it is noticeable that the auxiliary function $P(x)$ can improve the convergent properties of Fourier series.

2.2.2. Determining the expansion coefficients

Once the proper admissible function for the displacement field is selected Eq. (6), the next step is to find the expansion coefficients in the assumed displacement field. In order to do so Rayleigh-Ritz method is employed which is an energy-based method. To employ this method, it is necessary to state the potential and kinetic energies first in terms of displacement fields. The expression for the potential energy of the sector plate in local coordinates (s, ϕ, z) is derived from the constitutive laws and strain-displacement relations. According to the Mindlin plate theory. The strain energy of the annular sector plates can be expressed as:

$$U_p = \frac{1}{2} \int_0^\alpha \int_0^R D \left[\begin{array}{l} \left(\dfrac{\partial\theta_s}{\partial s}\right)^2 + \dfrac{2v}{(s+a)}\dfrac{\partial\theta_s}{\partial s}\left(\dfrac{\partial\theta_\phi}{\partial\phi}+\theta_s\right) + \dfrac{1}{(s+a)^2}\left(\dfrac{\partial\theta_\phi}{\partial\phi}+\theta_s\right)^2 \\ + \left(\dfrac{1-v}{2}\right)\dfrac{1}{(s+a)^2}\left(\theta_\phi - \dfrac{(s+a)\,\partial\theta_\phi}{\partial s} - \dfrac{\partial\theta_s}{\partial\phi}\right)^2 \\ + K^2 Gh\left[\left(\dfrac{\partial w_o}{\partial s}+\theta_s\right)^2 + \dfrac{1}{(s+a)^2}\left(\dfrac{\partial w_o}{\partial\phi}+(s+a)\theta_\phi\right)^2\right] \end{array} \right] (s+a)\,dsd\phi, \quad (11)$$

the kinetic energy expression for annular sector plate is expressed as:

$$T_p = \frac{1}{2}\omega^2 \int_0^\alpha \int_a^b \left(\rho h w_o{}^2 + \frac{\rho h^3}{12}(\theta_r{}^2 + \theta_\phi{}^2)\right) rdrd\phi. \quad (12)$$

The potential energy stored in the boundary springs is given by:

$$U_{sp} = \frac{1}{2}\left[\int_0^\alpha a\left[k_a w_o^2 + K_a^r \theta_s{}^2 + K_a^t \theta_\phi{}^2\right]_{s=0} + b\left[k_b w_o^2 + K_b^r \theta_s{}^2 + K_b^t \theta_\phi{}^2\right]_{s=R} d\phi \right.$$
$$+ \frac{1}{2}\int_0^R \left[\left[k_0 w_o^2 + K_0^r \theta_s{}^2 + K_0^t \theta_\phi{}^2\right]_{\phi=0} + \left[k_\alpha w_o^2 + K_\alpha^r \theta_s{}^2 + K_\alpha^t \theta_\phi{}^2\right]_{\phi=\alpha}\right] ds, \quad (13)$$

where k_a, k_b (k_0 and k_α) are linear spring constants, K_a^r, K_b^r (K_0^r and K_α^r) are rotational spring constants in radial direction, K_a^t, K_b^t (K_0^t and K_α^t) are rotational spring constants in tangential direction at edges $s = 0$ and $s = R$ and $\phi = 0$ and $\phi = \alpha$ respectively. All the classical homogeneous boundary conditions can be simply considered as special cases when the spring constants are either extremely large or substantially small. The units for the translational and rotational springs are N/m and Nm/rad, respectively.

After the potential and kinetic energies are expressed, then all the assumed displacement functions are inserted in the potential and kinetic energy equations and these equations are then further minimized with respect to the expansion coefficients in the displacement field. Mathematically, the Lagrangian for the annular sector plate can be generally expressed as:

$$L = U_p + U_{sp} - T_p, \tag{14}$$

where U_p is strain energy of the plate, U_{sp} is strain energy stored in the boundary springs and T_p is the kinetic energy of the plate. Substituting Eq. (6) in Eqs. (11)-(13) and then minimizing Lagrangian Eq. (14) against all the unknown series expansion coefficients that is:

$$\frac{\partial L}{\partial \Theta} = 0, \quad \text{where} \quad \Theta = A_{mn}, B_{mn}, C_{mn}, \tag{15}$$

we can obtain a series of linear algebraic expressions in a matrix form as:

$$(K - \omega^2 M)E = 0, \tag{16}$$

where E is a vector which contains all the unknown series expansion coefficients and K and M are the stiffness and mass matrices, respectively. E, K and M can be expressed as:

$$E = \left\{ \begin{matrix} A_{-2,-2}, A_{-2,-1}, A_{-2,0}, \dots, A_{m\prime,-2}, A_{m\prime,-1}, \dots A_{m\prime,n\prime}, \dots, A_{MN} \\ B_{-2,-2}, B_{-2,-1}, B_{-2,0}, \dots, B_{m\prime,-2}, B_{m\prime,-1}, \dots B_{m\prime,n\prime}, \dots, B_{MN} \\ C_{-2,-2}, C_{-2,-1}, C_{-2,0}, \dots, C_{m\prime,-2}, C_{m\prime,-1}, \dots C_{m\prime,n\prime}, \dots, C_{MN} \end{matrix} \right\}^T, \tag{17}$$

$$K = \begin{bmatrix} K_{ii}^p & K_{ij}^p & K_{ik}^p \\ K_{ji}^p & K_{jj}^p & K_{jk}^p \\ K_{ki}^p & K_{kj}^p & K_{kk}^p \end{bmatrix} + \begin{bmatrix} K_{ii}^{sp} & K_{ij}^{sp} & K_{ik}^{sp} \\ K_{ji}^{sp} & K_{jj}^{sp} & K_{jk}^{sp} \\ K_{ki}^{sp} & K_{kj}^{sp} & K_{kk}^{sp} \end{bmatrix}, \tag{18}$$

$$M = \begin{bmatrix} M_{ii} & 0 & 0 \\ 0 & M_{jj} & 0 \\ 0 & 0 & M_{kk} \end{bmatrix}, \tag{19}$$

where the subscripts i, j and k represents w, θ_s and θ_ϕ and the superscripts p and sp represents plate and boundary springs respectively. For conciseness, the detailed expressions for the stiffness and mass matrices are not shown here.

2.2.3. Determining the eigen values and eigen vectors

Once Eq. (16) is established, the eigenvalues (or natural frequencies) and eigenvectors of Mindlin annular sector plates can now be easily and directly determined from solving a standard matrix eigenvalue problem i.e. Eq. (16) using MATLAB. For a given natural frequency, the corresponding eigenvector actually contains the series expansion coefficients which can be used to construct the physical mode shape based on Eq. (6). Although this investigation is focused on the free vibration of Mindlin annular sector plate, the response of the annular sector plate to an applied load can be easily considered by simply including the work done by this load in the Lagrangian, eventually leading to a force term on the right side of Eq. (16).

3. Results and discussion

To check the accuracy and usefulness of the proposed technique, several numerical examples are presented in this section. It is important to mention here that the accuracy of the proposed method is greatly controlled by the number of truncation terms i.e. $M = N$, the more number of truncation terms we use we get more accurate results however the computational cost and time will increase with increasing number of truncation terms. Theoretically, there are infinite terms in the assumed displacement functions. However, the series is numerically truncated and finite terms are counted in actual calculations which will be further explained in the text to follow. Moreover, in identifying the boundary conditions in this section, letters C, S, and F have been used to indicate

the clamped, simply supported and free boundary condition along an edge, respectively. Therefore, the boundary conditions for a plate are fully specified by using four alphabets with the first one indicating the B.C. along the first edge, $r = a$. The remaining (the second to the fourth) edges are ordered in the counterclockwise direction.

First of all, in order to check the accuracy and usefulness we first consider a fully clamped Mindlin annular sector plate. Fully clamped (CCCC) boundary conditions can easily be achieved by setting the stiffnesses of the restraining springs to an infinitely large number (10^{14}) in the numerical calculations. The first six non-dimensional frequency parameter, $\Omega = \omega b^2 (\rho h / D)^{1/2}$ are tabulated in Table 1 along with the reference results from [9] and [27].

Table 1. First six non dimensional frequency parameter $\Omega = \omega b^2 (\rho h / D)^{1/2}$
for fully clamped (CCCC) Mindlin Annular sector plates ($\phi = 2\pi/3$, $a/b = 0.25$, $h/b = 0.2$)

$M = N$	Mode sequence					
	1	2	3	4	5	6
2	31.481	42.907	62.894	66.199	73.800	94.776
4	31.084	41.872	56.108	62.435	72.906	75.775
6	31.059	41.823	55.972	62.411	71.269	72.862
8	31.054	41.813	55.951	62.406	71.148	72.852
10	31.053	41.810	55.946	62.405	71.125	72.849
12	31.053	41.809	55.943	62.404	71.118	72.847
14	31.053	41.809	55.942	62.404	71.116	72.847
Ref. [9]	31.056	41.814	55.951	62.420	71.127	72.862
Ref. [27]	31.057	41.814	55.951	62.420	71.127	72.862

Similarly, in Table 2, first six non-dimensional frequency parameter for Mindlin annular sector plate having simply supported radial edges and clamped circumferential edges (CSCS) boundary conditions has been given along with the reference results from [9, 27]. A good agreement in the present values and reference values can be observed.

Table 2. First six non dimensional frequency parameter $\Omega = \omega b^2 (\rho h / D)^{1/2}$
for Mindlin Annular sector plates ($\phi = \pi/3$, $a/b = 0.5$, $h/b = 0.1$) having simply
supported radial edges and clamped circumferential edges (CSCS)

$M = N$	Mode sequence					
	1	2	3	4	5	6
2	77.625	104.054	161.254	170.932	194.112	243.145
4	76.567	102.955	149.795	166.952	190.467	215.603
6	76.476	102.765	149.410	166.772	190.093	206.703
8	76.449	102.696	149.323	166.726	189.961	206.315
10	76.439	102.667	149.290	166.710	189.908	206.228
12	76.435	102.654	149.275	166.703	189.883	206.196
14	76.432	102.647	149.267	166.699	189.871	206.182
Ref. [9]	76.902	103.682	150.413	167.327	191.593	207.276
Ref. [27]	76.902	103.682	150.413	167.327	191.593	207.276

Next we consider annular sector plate simply supported at radial edges and having different combination of boundary conditions (free-clamped, free-simply supported, simply supported-simply supported, simply supported-free and clamped-free) at the circumferential edges. The simply supported condition is simply produced by setting the stiffnesses of the translational and rotational springs to ∞ and 0, respectively, and the free edge condition by setting both stiffnesses to zero. The fundamental frequency parameters with different boundary conditions are shown in Table 3. The current results agree well with those taken from references [28, 29].

Next to illustrate the convergence and numerical stability of the current solution procedure, several sets of results for fully clamped Mindlin annular sector plates having different sector

angles and using different truncation numbers ($M = N = 2, 4, 6, 8, 10, 12, 14$) are presented in Tables 4-7. Furthermore, the fast convergence pattern can also be observed in Fig. 4.

Table 3. Fundamental frequency parameter $\Omega = \omega b^2 (\rho h/D)^{1/2}$ for Mindlin Annular sector plates having simply supported radial edges and different boundary conditions at circumferential edges ($a/b = 0.5$)

Sector angle (ϕ)	Thickness to radius ratio (h/b)	Method	Boundary conditions at circumferential edges				
			F-C	F-S	S-S	S-F	C-F
195	0.1	Present	19.998	10.224	38.365	4.560	12.696
		Ref. [28]	19.999	10.227	38.636	4.675	12.680
		Ref. [29]	20.097	10.239	38.764	–	–
	0.2	Present	17.503	9.130	32.508	4.005	11.413
		Ref. [28]	17.582	9.366	32.871	4.542	11.427
		Ref. [29]	17.764	9.396	33.190	–	–
210	0.1	Present	19.620	9.685	38.222	4.507	12.678
		Ref. [28]	19.610	9.664	38.455	4.584	12.659
		Ref. [29]	19.706	9.675	38.582	–	–
	0.2	Present	17.235	8.681	32.419	3.997	11.417
		Ref. [28]	17.294	8.877	32.734	4.458	11.425
		Ref. [29]	17.294	8.904	33.050	–	–
270	0.1	Present	18.654	8.213	37.868	4.392	12.639
		Ref. [28]	18.622	8.130	38.010	4.372	12.615
		Ref. [29]	18.715	8.139	38.134	–	–
	0..2	Present	16.548	7.450	32.200	3.999	11.433
		Ref. [28]	16.566	7.546	32.394	4.263	11.430
		Ref. [29]	16.739	7.567	32.704	–	–

A fast convergence pattern can be observed in the tabulated results as well as Fig. 4, therefore it can be concluded that sufficiently accurate results can be obtained with a small number of terms in the series expansion and the solution is consistently refined as more and more terms are included in the series expansion.

Table 4. First five non-dimensional frequency parameters $\Omega = \omega b^2 (\rho h/D)^{1/2}$ for CCCC Mindlin annular sector plates ($a/b = 0.6$, $h/b = 0.1$)

$M = N$	Sector angle	Mode sequence				
		1	2	3	4	5
2	$\phi = \dfrac{\pi}{6}$	145.584	240.451	251.723	331.721	391.843
4		144.104	237.420	249.040	328.660	350.364
6		144.032	237.301	248.941	328.487	349.816
8		144.020	237.280	248.924	328.452	349.739
10		144.017	237.274	248.920	328.442	349.720
12		144.016	237.272	248.918	328.438	349.713
14		144.015	237.271	248.917	328.436	349.711

Table 5. First five non-dimensional frequency parameters $\Omega = \omega b^2 (\rho h/D)^{1/2}$ for CCCC Mindlin annular sector plates ($a/b = 0.6$, $h/b = 0.1$)

$M = N$	Sector angle	Mode number				
		1	2	3	4	5
2	$\phi = \dfrac{\pi}{2}$	104.250	116.563	163.387	223.325	232.424
4		102.977	112.649	130.467	173.504	220.564
6		102.911	112.460	129.978	155.396	187.319
8		102.900	112.420	129.896	154.985	185.972
10		102.897	112.408	129.871	154.895	185.781
12		102.896	112.403	129.862	154.865	185.726
14		102.895	112.401	129.857	154.852	185.705

Table 6. First five non-dimensional frequency parameters $\Omega = \omega b^2 (\rho h/D)^{1/2}$ for CCCC Mindlin annular sector plates ($a/b = 0.6$, $h/b = 0.1$)

$M = N$	Sector angle	Mode number				
		1	2	3	4	5
2		102.797	109.453	139.708	221.999	227.027
4		101.566	106.400	115.457	143.396	194.321
6		101.503	106.239	115.077	128.766	147.504
8	$\phi = \dfrac{2\pi}{3}$	101.492	106.203	115.006	128.447	146.310
10		101.489	106.192	114.984	128.368	146.140
12		101.488	106.188	114.975	128.339	146.089
14		101.488	106.186	114.970	128.327	146.068

Table 7. First five non-dimensional frequency parameters $\Omega = \omega b^2 (\rho h/D)^{1/2}$ for CCCC Mindlin annular sector plates ($a/b = 0.6$, $h/b = 0.1$)

$M = N$	Sector angle	Mode sequence				
		1	2	3	4	5
2		101.717	103.774	115.254	220.887	222.496
4		100.537	101.885	104.287	114.756	138.302
6		100.480	101.779	104.088	107.716	113.103
8	$\phi = \dfrac{7\pi}{6}$	100.470	101.753	104.042	107.560	112.462
10		100.467	101.744	104.026	107.512	112.360
12		100.467	101.741	104.019	107.492	112.325
14		100.466	101.739	104.015	107.482	112.308

From Tables 4-7 it can be seen that when the truncated numbers change from $M \times N = 10 \times 10$ to 12×12, the maximum difference of the frequency parameters does not exceed 0.003 for the worst case, which is acceptable. Furthermore, in modal analysis the natural frequencies for higher order modes tend to converge slower as compared to the lower order modes which can easily be observed in Fig. 4 that the 9th mode frequency converges slowly as compared to the 6th and 3rd mode. Thus a suitable truncation number should be used to achieve the accuracy of the largest desired natural frequency. In view of above and excellent numerical behavior of the current solution, the truncation number for all subsequent calculations in the present method is taken as $M = N = 12$.

Next we study the effect of sector angle and thickness-radius ratio and cutout ratio on non-dimensional frequency parameter. The effect has been graphically represented in Figs. 5-7, respectively.
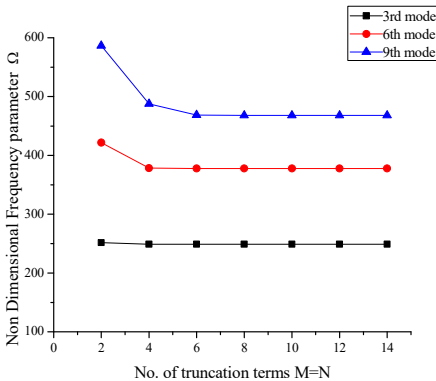

Fig. 4. Convergence pattern of frequency parameters with no. of terms ($M = N$)
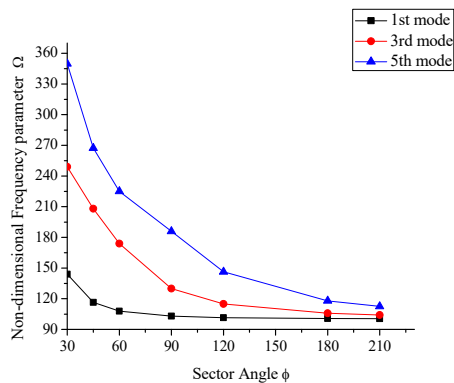

Fig. 5. Effect of sector angle on non-dimensional frequency parameter 'Ω'
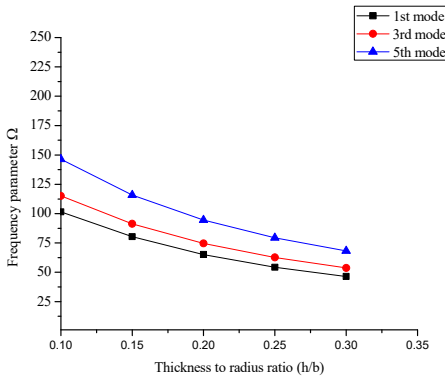
Fig. 6. Effect of thickness to radius ratio (h/b) on the frequency parameter
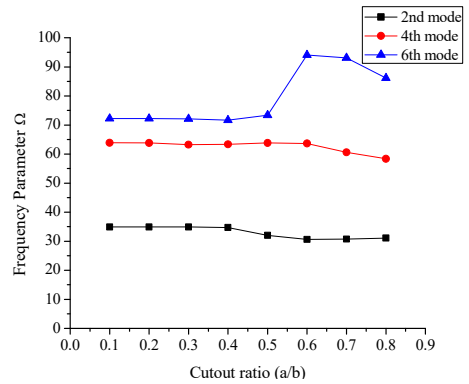
Fig. 7. Effect of cutout ratio (a/b) on the frequency parameters

It can be seen in Fig. 5 that for smaller sector angles i.e. $\phi \leq 2\pi/3$, the decrease in the frequency parameters is more as compared to the sector angles greater than $2\pi/3$. Similarly, in figure 6, 1st, 3rd and 5th mode frequency parameters have been plotted against different thickness to radius ratios (h/b) for a fully clamped (CCCC) Mindlin annular sector plate having sector angle = $2\pi/3$ and cutout ratio = $a/b = 0.6$. It can be observed that with the increase in thickness to radius ratio the frequency parameter always decreases. Similarly, the effect of cutout ratio i.e. inner radius to outer radius (a/b) on the frequency parameters for a FSFS mindlin annular sector plate having sector angle = $\pi/3$, and $h/b = 0.2$ can be seen in Fig. 7.

As mentioned previously, using this method, a Mindlin circular sector plate can also be analyzed easily just by equating the inner radius of Mindlin annular sector plate to zero without modifying the equations or the solution algorithm. Table 8 shows first six non-dimensional frequency parameter along with reference results for Mindlin circular sector plates having inner radius = $a = 0.0001$, different thickness to radius ratio and sector angles and subjected to simply supported radial edges and clamped circular edge (SCS) boundary condition respectively. A close agreement can be observed in the present values and the reference results.

Table 8. First six non-dimensional frequency parameters
for SCS Mindlin Circular sector plates ($a/b = 0.0001$)

Sector angle (ϕ)	Thickness to radius ratio (h/b)	Method	Mode sequence					
			1	2	3	4	5	6
$\frac{\pi}{6}$	0.1	Present	91.419	148.357	205.117	208.046	278.356	281.097
		Ref. [8]	93.450	152.630	206.900	213.080	274.650	283.190
	0.2	Present	66.272	98.992	131.454	131.981	161.648	163.749
		Ref. [8]	67.933	102.560	132.860	135.610	165.680	167.820
$\frac{\pi}{2}$	0.1	Present	31.657	60.112	71.009	92.956	110.151	118.760
		Ref. [8]	32.205	60.637	72.221	93.450	111.320	120.450
	0.2	Present	26.298	46.323	53.227	67.436	77.370	82.512
		Ref. [8]	26.993	46.906	54.466	67.933	78.582	83.903
π	0.1	Present	20.778	31.969	45.586	54.582	60.614	71.698
		Ref. [8]	20.223	32.205	45.773	53.859	60.637	72.221
	0..2	Present	17.752	26.630	36.470	42.169	46.726	53.813
		Ref. [8]	17.773	26.993	36.758	42.393	46.906	54.466
$\frac{7\pi}{6}$	0.1	Present	19.915	28.398	39.635	51.986	52.898	65.557
		Ref. [8]	19.489	28.599	39.786	51.998	52.416	65.091
	0.2	Present	16.871	23.958	32.269	40.788	40.916	49.836
		Ref. [8]	17.092	24.293	32.519	41.067	41.195	49.859

All the examples mentioned above are limited to different combinations of classical boundary

conditions which are viewed as special case of elastically restrained edges. After verifying the convergence, accuracy and effectiveness of the proposed method for different combinations of classical boundary conditions, the method is further employed here to study the vibration characteristics of Mindlin annular sector and circular sector plates subjected to general elastic boundary conditions.

In order to simulate the elastic boundary conditions, it is important to study the effect of restraining springs first on the frequency parameters so that proper value to the restraining springs could be assigned. Fig. 8 shows the effect of restraining springs stiffness on the frequency parameter for Mindlin annular sector plate ($a/b = 0.6$, $h/b = 0.2$ and $\phi = 120$).

Fig. 8 shows 1st, 5th and 10th mode frequency parameters plotted against the spring stiffnesses by varying the stiffnesses of one group of boundary spring from 0 to 10^{16} while keeping the stiffnesses of the other group equal to infinite i.e 10^{16}. It can be seen in Fig. 8(a) that the frequency parameter almost remains at a level when the stiffness of the translational spring in z direction is less than 10^8 and greater than 10^{12} where as other than this range the frequency parameter increases with increasing stiffness values. Similar phenomena can be observed in case of rotational spring stiffness however a slight change in frequency parameter can be observed with in the stiffness range from 10^8 to 10^{10}. Based on the analysis it can be concluded that stable frequency parameter can be obtained when the stiffnesses for all the restraining springs is more than 10^{12} or less than 10^8 and also it is suitable and valid to use the stiffness value 10^{14} to simulate the infinite stiffness in the numerical calculations since the frequency parameter remain at the same level for values greater than equal to 10^{14}. It can also be concluded that the elastic stiffness range for translational spring is more than the two rotational springs.
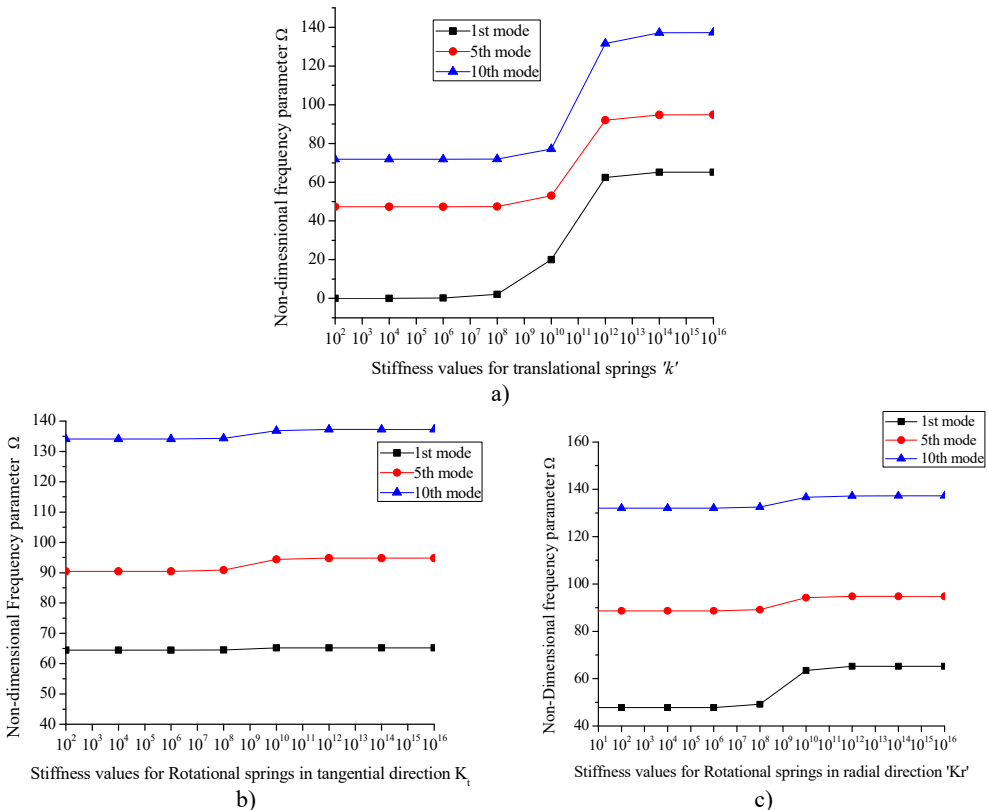

Fig. 8. a) Effect of translational spring stiffness (k) on Ω, and effect of rotational spring stiffness b) in tangential direction (Kt) on Ω, c) in radial direction (Kr) on Ω

From Fig. 8, an elastic boundary condition can easily be defined with any stiffness value between 10^8 to 10^{12}. To the author's best knowledge, no reported results are available in literature for vibration analysis of Mindlin annular sector plates under general elastic boundary conditions. As mentioned earlier the present method can be used to obtain natural frequency parameters for Mindlin annular sector plates under general elastic boundary condition regardless of modifying solution algorithm and procedure.

In order to achieve valuable results for annular sector plates subjected to elastic boundary conditions, we define an elastic restraint 'E^1' having corresponding translational and rotational spring stiffness values $k = 1e8$, $K_r = 0$ and $K_t = 0$. Tables 9-11 shows first five natural frequency parameters for Mindlin annular sector plates having different sector angles and thickness-radius ratio (h/b) subjected to E^{1}E^{1}E^{1}E^1, FE^1 FE^1 and CE^{1}CE^1 boundary conditions where E^{1}E^{1}E^{1}E^1, FE^1 FE^1 and CE^{1}CE^1 represents the combination of classic and elastic boundary conditions at edges a and b as well as $\phi = 0$ and α.

Due to unavailability of results in previous literature for these types of boundary conditions (E^{1}E^{1}E^{1}E^1, FE^1 FE^1 and CE^{1}CE^1), the comparison has been made with results obtained from ABAQUS. However, we know that the core algorithm of the ABAQUS software is based on the finite element method. Furthermore, the FEM computational accuracy strongly depends on the size of the mesh and the type of element selection. For more accuracy in the higher frequency region and for complex geometries, a highly refined mesh and a higher order finite element is needed. We know that the smaller the mesh size, the greater the number of elements we get for analysis which further requires more computer memory and subsequently a high computational cost. Since the geometry under investigation in this manuscript is a simpler geometry therefore a simple free meshing technique with mesh size 0.005 and S4R (Shell 4 node Reduced Integration) element type has been used which is computationally inexpensive and is considered suitable for this type of geometry and modal analysis. Keeping the mesh size 0.005, the number of elements used in the analysis for annular sector plate having sector angle $\pi/3$, $\pi/2$, $2\pi/3$ and π are 13040, 20080, 29727 and 40240 respectively.

A very good agreement can be observed in Tables 9-11 between the calculated results and the one obtained from ABAQUS. This shows that the present method can be easily applied to classical and elastic type boundary conditions as well as their combination without modifying the solution algorithm and procedure. The results tabulated in Tables 9-11 can be used as a bench mark for future computational methods.

Table 9. First five natural frequency parameters for Mindlin Annular sector plates subjected to E^{1}E^{1}E^{1}E^1 type elastic boundary conditions ($a/b = 0.6$)

Sector angle (ϕ)	Thickness to radius ratio (h/b)	Method	Natural frequency modes				
			1	2	3	4	5
$\dfrac{\pi}{3}$	0.1	Present	337.934	435.140	506.867	1520.326	1966.903
		ABAQUS	337.690	437.350	507.130	1522.500	1969.600
	0.2	Present	241.050	302.391	330.646	2587.184	3074.622
		ABAQUS	240.970	303.960	330.420	2590.100	3080.200
$\dfrac{\pi}{2}$	0.1	Present	314.276	389.282	479.851	870.662	1294.086
		ABAQUS	313.770	390.700	480.060	872.380	1295.400
	0.2	Present	225.655	274.476	318.276	1411.322	1991.271
		ABAQUS	225.400	275.570	318.090	1412.500	1994.500
$\dfrac{2\pi}{3}$	0.1	Present	300.548	361.101	440.420	703.848	884.878
		ABAQUS	301.310	364.010	443.800	707.710	901.740
	0..2	Present	216.209	257.039	302.020	1032.654	1342.753
		ABAQUS	216.710	259.290	303.580	1037.500	1374.000
π	0.1	Present	288.597	325.207	378.969	516.005	622.710
		ABAQUS	288.110	325.230	380.110	517.160	622.670
	0.2	Present	206.659	235.054	270.651	650.104	811.858
		ABAQUS	206.290	235.350	271.530	650.900	811.980

Table 10. First five natural frequency parameters for Mindlin Annular sector plates subjected to FE^{1}FE^1 type elastic boundary conditions ($a/b = 0.4$)

Sector angle (ϕ)	Thickness to radius ratio (h/b)	Method	Natural frequency				
			1	2	3	4	5
$\frac{\pi}{3}$	0.1	Present	119.832	264.818	319.661	1483.220	1916.028
		ABAQUS	119.940	264.970	319.570	1484.100	1917.400
	0.2	Present	83.397	180.756	222.669	2577.428	3060.712
		ABAQUS	83.395	180.750	222.710	2580.000	3066.200
$\frac{\pi}{2}$	0.1	Present	57.023	251.087	267.380	786.925	1222.649
		ABAQUS	56.935	251.210	267.440	787.520	1223.700
	0.2	Present	41.696	179.512	185.090	1389.419	1971.191
		ABAQUS	40.802	179.550	184.680	1390.300	1974.300
$\frac{2\pi}{3}$	0.1	Present	24.833	201.973	271.669	561.948	806.253
		ABAQUS	24.039	202.070	271.430	562.430	806.550
	0.2	Present	18.952	149.812	189.712	995.529	1318.058
		ABAQUS	17.523	149.840	189.290	995.930	1319.700
π	0.1	Present	3.867	120.269	233.439	411.437	434.108
		ABAQUS	3.856	120.260	233.370	411.390	434.060
	0.2	Present	3.869	105.112	171.054	610.370	758.047
		ABAQUS	0.000	105.100	170.900	610.820	758.160

4. Conclusion

An improved Fourier series method has been presented for vibration analysis of moderately thick annular and circular sector plates with classical and general elastic restraints along its edges. Regardless of the boundary conditions, the displacement function is invariantly expressed as an improved trigonometric series which converges uniformly at an accelerated rate. The efficiency, accuracy and reliability of the present method have been fully demonstrated by various numerical examples for moderately thick annular sector plates having different cutout ratios and sector angles.

Table 11. First five natural frequency parameters for Mindlin Annular sector plates subjected to CE^{1}CE^1 type elastic boundary conditions ($a/b = 0.4$)

Sector angle (ϕ)	Thickness to radius ratio (h/b)	Method	Natural frequency modes				
			1	2	3	4	5
$\frac{\pi}{3}$	0.1	Present	5161.242	5329.372	6024.050	7500.647	9771.648
		ABAQUS	5182.600	5349.600	6044.000	7521.400	8046.600
	0.2	Present	6628.586	6823.656	7744.270	9710.654	12411.918
		ABAQUS	6665.600	6859.200	7778.100	9746.900	10565.000
$\frac{\pi}{2}$	0.1	Present	5167.620	5242.262	5540.684	6140.785	7122.635
		ABAQUS	5188.700	5261.800	5560.000	6158.100	7141.200
	0.2	Present	6633.347	6724.016	7105.490	7936.324	9269.663
		ABAQUS	6673.500	6762.800	7142.300	7970.700	9306.600
$\frac{2\pi}{3}$	0.1	Present	5171.158	5212.374	5378.060	5694.631	6205.673
		ABAQUS	5191.900	5231.300	5397.000	5711.500	6222.000
	0..2	Present	6636.080	6687.398	6895.770	7327.756	8047.005
		ABAQUS	6676.100	6726.100	6933.100	7362.200	8080.800
π	0.1	Present	5175.030	5192.529	5265.762	5397.220	5599.831
		ABAQUS	5195.000	5210.600	5284.500	5414.600	5616.400
	0.2	Present	6639.126	6661.568	6752.481	6926.255	7207.997
		ABAQUS	6678.800	6699.900	6790.300	6961.700	7241.800

The effect of sector angle, thickness to radius ratio and restraining springs on the frequency parameters has been discussed. The present method is also employed to study the vibration

analysis of moderately thick circular sector plates without modifying the solution procedure. Results for moderately thick annular sector plates under general elastic boundary conditions for various thicknesses to radius ratio and sector angle are presented which can serve as a bench mark for future computational methods. The accuracy of the results has been verified by comparing it with those available in literature and with ABAQUS. An excellent agreement is observed between the results obtained using the present method and with those available in literature. Keeping in view the accuracy and fast convergence behavior this method can easily be further extended to study the vibration analysis of various built up structures without modifying the solution algorithm and procedure.

Acknowledgements

References

[1] **Guruswamy P., Yang T. Y.** A sector element for dynamic analysis of thick plates. Journal of Sound and Vibration, Vol. 62, 1979, p. 505-516.

[2] **Soni S. R., Amba Rao C. L.** On radially symmetric vibrations of orthotropic non uniform disks including shear deformation. Journal of Sound and Vibration, Vol. 42, 1975, p. 57-63.

[3] **Liew K. M., Xiang Y., Wang C. M., Kitipornchai S.** Flexural vibration of shear deformable circular and annular plates on ring supports. Computer Methods in Applied Mechanics and Engineering, Vol. 110, 1993, p. 301-315.

[4] **Liew K. M., Xiang Y., Kitipornchai S., Wang C. M.** Buckling and vibration of annular Mindlin plates with internal concentric ring supports subject to in-plane radial pressure. Journal of Sound and Vibration, Vol. 177, Issue 5, 1994, p. 689-707.

[5] **Cheung M. S., Chan M. Y. T.** Static and dynamic analysis of thin and thick sectorial plates by the finite strip method. Computers and Structures, Vol. 14, 1981, p. 79-88.

[6] **Srinivasan R. S., Thiruvenkatachari V.** Free vibration of transverse isotropic annular sector Mindlin plates. Journal of Sound and Vibration, Vol. 101, 1985, p. 193-210.

[7] **Mizusawa T.** Vibration of thick annular sector plates using semi analytical methods. Journal of Sound and Vibration, Vol. 150, 1991, p. 245-259.

[8] **Liu F. L., Liew K. M.** Free vibration analysis of Mindlin sector plates: numerical solutions by differential quadrature methods. Computer Methods in Applied Mechanics and Engineering, Vol. 177, 1999, p. 77-92.

[9] **Liew K. M., Liu F. L.** Differential quadrature method for free vibrations of shear deformable annular sector plates. Journal of Sound and Vibrations, Vol. 230, Issue 2, 2000, p. 335-356.

[10] **Wu T. Y., Liu G. R.** Free vibration analysis of circular plates with variable thickness by the generalized differential quadrature rule. International Journal of Solid and Structures, Vol. 38, 2001, p. 7967-7980.

[11] **Xiang Y., Zhang L.** Free vibration analysis of stepped circular Mindlin plates. Journal of Sound and Vibration, Vol. 280, 2005, p. 633-655.

[12] **So J., Leissa A. W.** Three dimensional vibrations of thick circular and annular plates. Journal of Sound and Vibration, Vol. 209, 1998, p. 15-41.

[13] **Hashemi S. H., Tahir H. R. D., Omidi M.** 3-D free vibration analysis of annular plates on Pasternak elastic foundation via p-Ritz method. Journal of Sound and Vibration Vol. 311, 2008, p. 1114-1140.

[14] **Liew K. M., Yang B.** Elasticity solutions for free vibrations of annular plates from three-dimensional analysis. International Journal of Solids and Structure, Vol. 37, 2000, p. 7689-7702.

[15] **Zhou D., Au F. T. K., Cheung Y. K., Lo S. H.** Three dimensional vibration analyses of circular and annular plates via the Chebyshev-Ritz method. International Journal of Solid and Structures Vol. 40, 2003, p. 3089-3105.

[16] **Farag N. H., Pan J.** Modal characteristics of in-plane vibration of circular plates clamped at the outer edge. Journal of Acoustical society of America, Vol. 113, Issue 4, 2003.

[17] **Karamooz Ravari M. R., Forouzan M. R.** Frequency equations for the in-plane vibration of orthotropic circular annular plates. Archives of Applied Mechanics, Vol. 81, 2010, p. 1307-1322.

[18] **Li W. L.** Free vibrations of beams with general boundary conditions. Journal of Sound and Vibration, Vol. 237, 2000, p. 709-725.

[19] **Li W. L.** Comparison of Fourier sine and cosine series expansions for beams with arbitrary boundary conditions. Journal of Sound and Vibration, Vol. 255, Issue 1, 2002, p. 185-194.

[20] **Li W. L., Bonilha M. W., Xiao J.** Vibrations of two beams elastically coupled together at an arbitrary angle. Acta Mechanica Solida Sinica, Vol. 25, 2012, p. 61-72.

[21] **Li W. L.** Vibration analysis of rectangular plates with general elastic boundary supports. Journal of Sound and Vibration, Vol. 273, 2004, p. 619-635.

[22] **Li W. L., Zhang X., Du J., Liu Z.** An exact series solution for the transverse vibration of rectangular plates with general elastic boundary supports. Journal of Sound and Vibration, Vol. 321, 2009, p. 254-269.

[23] **Shi D. Y., Shi X. J., Li W. L., Wang Q. S.** Free transverse vibrations of orthotropic thin rectangular plates with arbitrary elastic edge supports. Journal of Vibroengineering, Vol. 16, 2014, p. 389-398.

[24] **Shi Xianjie, Shi Dongyan, Qin Zhengrong, Wang Qingshan** In-plane vibration analysis of annular plates with arbitrary boundary conditions. The Scientific World Journal, 2014.

[25] **Shi Xianjie, Kong Lingcheng, Shi Dongyan, Li Wen L.** Three-dimensional vibration analysis of annular sector plates with arbitrary thicknesses and Boundary conditions. Inter Noise, Innsbruck, Austria, 2014.

[26] **Shi Xianjie, Shi Dongyan, Li Wen L., Wang Qingshan** A unified method for free vibration of circular, annular and sector plates with arbitrary boundary conditions. Journal of Vibration and Control, 2014.

[27] **Ma'en Sari S.** Free vibration analysis of non-local annular sector Mindlin plates. International Journal of Mechanical Sciences, Vols. 96-97, 2015, p. 25-35.

[28] **Zhou D., Lo S. H., Cheung Y. K.** 3-D vibration analysis of annular sector plates using the Chebyshev-Ritz method. Journal of Sound and Vibration Vol. 320, 2009, p. 421-437.

[29] **Mcgee O. G., Huang C. S., Leissa A. W.** Comprehensive exact solutions for free vibrations of thick annular sectorial plates with simply supported radial edges. International Journal of Mechanical Sciences, Vol. 37, Issue 5, 1995, p. 537-566.

Fazl e Ahad received Master's degree in Mechanical Engineering Design from University of Engineering and Technology Peshawar Pakistan. Presently pursuing Ph.D. from Harbin Engineering University, China in the field of mechanical design and theory. Research field includes vibrations of structures.

Dongyan Shi is a Professor in School of Mechanical and Electrical Engineering, Harbin Engineering University, China. Her research field includes modern mechanical design theory and method, mechanism and structure strength.

Zarnab Hina completed her Bachelor in Telecommunication Engineering from University of Engineering and Technology Taxila, Pakistan. Presently she is pursuing Masters in Information and Communication Engineering from Harbin Engineering University China. Major research interest field includes optical orthogonal frequency division multiplexing.

Syed M. Aftab completed his Bachelor in Mechanical Engineering from NED University Karachi, Pakistan. Presently he is pursuing Masters in mechanical engineering from Harbin Engineering University. His research field includes structural vibrations.

Hafiz M. Waqas completed his bachelor in Mechanical Engineering from National University of Science and Technology Pakistan. Presently he is pursuing masters in mechanical engineering from Harbin Engineering University. His research field includes tensegrity structures.